

RESEARCH

Open Access



The comprehensive profile of fermentation products during in situ CO₂ recycling by Rubisco-based engineered *Escherichia coli*

Cheng-Han Yang, En-Jung Liu, Yi-Ling Chen, Fan-Yu Ou-Yang and Si-Yu Li*

Abstract

Background: In our previous study, the feasibility of Rubisco-based engineered *E. coli* (that contains heterologous phosphoribulokinase (PrkA) and Rubisco) for in situ CO₂ recycling during the fermentation of pentoses or hexoses was demonstrated. Nevertheless, it is perplexing to see that only roughly 70 % of the carbon fed to the bacterial culture could be accounted for in the standard metabolic products. This low carbon recovery during fermentation occurred even though CO₂ emission was effectively reduced by Rubisco-based engineered pathway.

Results: In this study, the heterologous expression of form I Rubisco was found to enhance the accumulation of pyruvate in *Escherichia coli* MZLF [*E. coli* BL21(DE3) Δzwf , Δldh , Δfrd]. This may be attributed to the enhanced glycolytic reaction supported by the increased biomass and the ethanol/acetate ratio. Besides, it was found that the transcription of *arcA* (encodes the redox-dependent transcriptional activators ArcA that positively regulates the transcription of pyruvate formate-lyase) was down-regulated in the presence of Rubisco. The enhanced accumulation of pyruvate also occurs when PrkA is co-expressed with Rubisco in *E. coli* MZLF. Furthermore, *E. coli* containing Rubisco-based engineered pathway has a distinct profile of the fermentation products, indicating CO₂ was converted into fermentation products. By analyzing the ratio of total C-2 (2-carbon fermentation products) to total C-1 (1-carbon fermentation product) of MZLFB (MZLF containing Rubisco-based engineered pathway), it is estimated that 9 % of carbon is directed into Rubisco-based engineered pathway.

Conclusions: Here, we report for the first time the complete profile of fermentation products using *E. coli* MZLF and its derived strains. It has been shown that the expression of Rubisco alone in MZLF enhances the accumulation of pyruvate. By including the contribution of pyruvate accumulation, the perplexing problem of low carbon recovery during fermentation by *E. coli* containing Rubisco-based engineered pathway has been solved. 9 % of glucose consumption is directed from glycolysis to Rubisco-based engineered pathway in MZLFB. The principle characteristics of mixotroph MZLFB are the high bacterial growth and the low CO₂ emission.

Keywords: The Calvin–Benson–Bassham (CBB) cycle, Ribulose-1,5-bisphosphate carboxylase/oxygenase (Rubisco), Pyruvate, Mixotroph

Background

The Calvin–Benson–Bassham (CBB) cycle, also known as the reductive pentose phosphate cycle, is a metabolic

pathway involving the conversion of three molecules of carbon dioxide into one molecule of glyceraldehyde-3-phosphate. The CBB cycle uses 11 enzymes to complete autotrophic CO₂ fixation. Interestingly, most of enzymes are also involved in the central metabolism including glycolysis and the pentose phosphate pathway. Therefore, it is generally accepted that the functional CBB cycle that

*Correspondence: syli@dragon.nchu.edu.tw
Department of Chemical Engineering, National Chung Hsing University,
Taichung 402, Taiwan

emerged billions of years ago did not evolved as a whole, but instead the individual enzymes have their own phylogenetic history that is independent of the biochemical distribution of the CBB cycle [1]. Consequently, one way to genetically assess whether a microorganism utilizes the CBB cycle is to characterize the manifestation of two key genes that encodes phosphoribulokinase (PRK) and Ribulose-1,5-bisphosphate carboxylase/oxygenase (Rubisco). Rubisco is the one enzyme that is specific to the CBB cycle. Rubisco catalyzes the carboxylation and the oxygenation of ribulose-1,5-bisphosphate with CO₂ and O₂, respectively. The products of carboxylation and oxygenation are 3-phosphoglycerate and 2-phosphoglycolate and the former will be sequentially converted into glyceraldehyde-3-phosphate by phosphoglycerate kinase and glyceraldehyde-3 phosphate dehydrogenase whereas the latter will enter photorespiration [2].

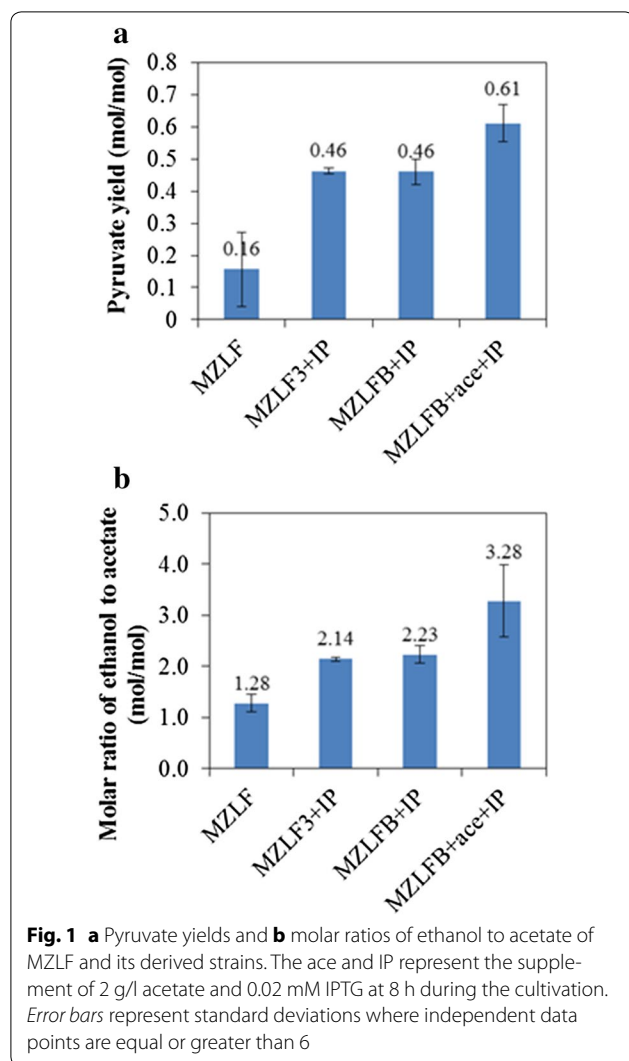
The CBB cycle has been used in the engineering perspective for converting CO₂ into bio-based chemicals. For example, microalgae have been used to produce carbohydrates from CO₂, where the carbohydrates produced were subsequently used for bioethanol production [3]. A sequential fermentation process was proposed for a hydrogen production process with zero CO₂ emission [4]. Cyanobacteria have been engineered to produce various bio-based chemicals from autotrophic CO₂ assimilation [5–8]. On the other hand, PRK and Rubisco without the function of the full CBB cycle were shown to improve oil production in developing embryos of *Brassica napus* L [9]. This partial CBB cycle was also developed in Rubisco-dependent *Escherichia coli* (RDE) for the selection of Rubisco mutants that had better performance in terms of reaction rate and CO₂/O₂ selectivity [10–13]. The quantitative analysis of CO₂ fixation in recombinant *E. coli* has been reported recently where 17 % of carbon was found to be directed to Rubisco-based engineered pathway in the presence of the carbonic anhydrase [14]. In our previous study, the feasibility of Rubisco-based engineered *E. coli* for in situ CO₂ recycling during the fermentation of pentoses was demonstrated [15]. By enhancing the function of the homologous non-oxidative pentose phosphate pathway, Rubisco-based engineered *E. coli* can be further used to achieve a low CO₂ emission during the fermentation of hexoses [16]. While Rubisco-based engineered pathway (that contains PrkA and Rubisco) is arguably compatible to the central metabolism of *E. coli* [16], it is perplexing to see the enhanced biomass accumulation and other physiological responses when form I Rubisco is heterologously expressed in *E. coli* [15]. It is also perplexing to see that only roughly 70 % of the carbon fed to the bacterial culture could be accounted for in the standard metabolic products. This low carbon recovery (the carbon recovery is defined as the mole of carbon of total

fermentation products/the mole of carbon of consumed glucose) during fermentation occurred even though CO₂ emission was effectively reduced by Rubisco-based engineered pathway [15, 16]. The low carbon recovery of 73 % can be seen for MZLFB + IP when pyruvate was not included for the calculation, see below. This unforeseen carbon distribution is also observed when Rubisco-based engineered pathway is heterologously expressed in *Saccharomyces cerevisiae* [17]. In this study, a recombinant *E. coli* strain with the deactivations of *ldh* and *frd* genes (encoding the lactate dehydrogenase and the fumarate reductase, respectively) was constructed to study the partition of carbon flow among the wild-type fermentation routes and Rubisco-based engineered pathway was quantified by examining the profiles of the end-metabolites. During which, several interesting phenotypes due to the overexpression of form I Rubisco were presented. Finally, the feasibility of mixotrophic *E. coli* as a platform for bio-based chemical productions was discussed.

Results and discussion

The pyruvate accumulation was found to be enhanced in *E. coli* in the presence of Rubisco

It is consistently found from previous literature [15–17] that the carbon recovery generally decreased when Rubisco was heterologously expressed. This appears to diminish the usefulness of Rubisco for biotechnology applications. To investigate the carbon flow in *E. coli* strain containing Rubisco-based engineered pathway, *E. coli* strain MZLF, derived from *E. coli* strain MZ (*E. coli* BL21(DE3) Δzwf [16]), was firstly constructed by deleting the non-lethal *ldh* and *frd* genes. Note that *zwf*, *ldh*, and *frd* genes encode glucose-6-phosphate 1-dehydrogenase, lactate dehydrogenase, and fumarate reductase, respectively. It can be seen in Fig. 1a that pyruvate was one of the major fermentation products for MZLF where the molar yield was 0.16, accounting for 9 % of the total carbon recovery (see data below). When the overexpression of Rubisco was achieved by the addition of isopropyl- β -D-1-thiogalactopyranoside (IPTG) during anaerobic culture of *E. coli* strains MZLF3 in M9 medium, a more than 2-fold increase in the yield of pyruvate can be observed. This unexpected result from MZLF3 was reproduced when MZLFB (MZLF containing *rbclS* and *prkA*) was tested. The pyruvate yield can be increased by another 33 % by the addition of 30 mM acetate. Therefore, it can be concluded that it is Rubisco that induces the physiological response in *E. coli* MZLF and one of the main products is pyruvate. Note that an non-active Rubisco can also lead to the enhanced pyruvate production but not the CO₂ assimilation, see below. This is consistent with our previous study that Rubisco alone can stimulate different physiological responses (enhanced biomass production and more) in *E.*



coli as discussed in Introduction [15, 16]. It is also interesting to see in Fig. 1b that the overexpression of Rubisco led to a significant increase in the molar ratio of ethanol to acetate. While the molar ratio of ethanol to acetate for MZLF was 1.28, increases to 2.14 and 2.23 were respectively found for MZLF3 + IP and MZLFB + IP. A more than twofold increase from 1.34 to 3.28 was reported for MZLFB + ace + IP. Table 1 summarizes bacterial strains and plasmids used in this study. It should be noted that Rubisco used in MZLF3 or MZLFB is a mutant evolved from Rubisco of *Synechococcus* PCC6301 [13]. Nevertheless, we have shown that wild-type Rubisco also induced the pyruvate accumulation with a molar yield of 0.44 mol/mol-glucose (data not shown). Note that the elementary biomass composition of $\text{CH}_{1.77}\text{O}_{0.49}\text{N}_{0.24}$ is used for the calculations of carbon recovery and molar yield [18].

The distribution of C-2 fermentation products (i.e., ethanol and acetate) partly reflects the intracellular balances

of ATP and the reducing equivalents. It has been demonstrated that the glycolytic flux is mainly controlled by the demand for ATP during the anaerobic growth of *E. coli* in the minimal medium [19, 20]. When the ATP demand, resulting from the anabolism, is strong and intense, the glycolic flux will accordingly increase to replenish ATP supply by the substrate-level phosphorylation. Moreover, additional ATP production can be achieved by the conversion of pyruvate derived from glycolysis. However, this route for the additional ATP production is restrained by surplus reducing equivalents generated from glycolysis where the conversion of pyruvate to ethanol is one of the main mechanisms to respire the reducing equivalents. The increase in the molar ratio of ethanol to acetate as shown in Fig. 1b infers that NADH may be produced in excess when Rubisco was overexpressed (see MZLF3 + IP). The introduction of PrkA in MZLFB (containing both Rubisco and PrkA), representing the extra demand for ATP, resulted in an additional increase of the ethanol:acetate ratio from 2.14 to 2.23 for MZLFB + IP. It is therefore suggested that the overproduction of NADH may result from an increase in glycolysis, which is because of the high demand for ATP in MZLF3 + IP and MZLFB + IP. These observations are consistent with the results when 30 mM of acetate were added, further increasing the molar ratio of ethanol to acetate from 2.23 to 3.28. The addition of acetate lowered the conversion of pyruvate to acetate by roughly 40 % (data not shown). The reduced acetate production resulted in reduced ATP production, thus further stimulating the glycolytic pathway to some extent. Note that the addition of 30 mM acetate during the cultivation of MZLF provided a pyruvate yield of 0.13 and an ethanol/acetate ratio of 1.25 (data not shown). This relatively same performance compared to MZLF as shown in Fig. 1 indicates that the enhanced pyruvate production observed for MZLFB + ace + IP (Fig. 1a) is because of the presence of Rubisco. And the enhanced pyruvate production can be attributed to the unbalanced ATP production. The enhanced glycolytic activity accompanied by enhanced bacterial growth is consistent with our previous study when Rubisco was aerobically overexpressed in *E. coli* BL21 (DE3) [15].

Pyruvate is not a typical fermentation product of anaerobic cultivation of *E. coli*. Instead, it is an important metabolic node that is associated with the metabolisms of lactate, acetate, ethanol, and succinate [21]. It is also involved in the anaplerosis (through phosphoenolpyruvate-pyruvate-oxaloacetate) as well as glucose metabolism (through phosphotransferase system, PTS) [22]. The enhanced glycolysis due to the overexpression of Rubisco should lead to vigorous function of PTS where PEP is converted to pyruvate. At the same time, the enhanced anaplerotic metabolism has been shown

Table 1 List of bacterial strains and plasmids used in this study

Name	Descriptions	Reference
<i>Bacterial strains</i>		
<i>E. coli</i> BL21 (DE3)	F ⁻ , <i>dcm</i> , <i>ompT</i> , <i>gal</i> , <i>lon</i> , <i>hsdS_B</i> (rB ⁻ , mB ⁻), λ (DE3[<i>lacI</i> , <i>lacUV5</i> -T7 gene 1, <i>ind1</i> , <i>sam7</i> , <i>nin5</i>])	Lab stock
J3	<i>E. coli</i> BL21 (DE3) harboring <i>rbclS</i> -pET30a + (M259T)	[15]
JB	<i>E. coli</i> BL21 (DE3) harboring both P _{BAD} - <i>his6-prkA</i> -pACYC184 and <i>rbclS</i> -pET30a + (M259T)	[15]
MZ	<i>E. coli</i> BL21 (DE3) Δ <i>zwf</i>	[16]
MZL	MZ, Δ <i>ldh</i>	This study
MZLF	MZL, Δ <i>frd</i>	This study
MZLF1	MZLF harboring P _{BAD} - <i>his6-prkA</i> -pACYC184	This study
MZLF3	MZLF harboring <i>rbclS</i> -pET30a + (M259T)	This study
MZLFB	MZLF harboring both P _{BAD} - <i>his6-prkA</i> -pACYC184 and <i>rbclS</i> -pET30a + (M259T)	This study
<i>Plasmids</i>		
pKD46	<i>araC</i> , <i>bla</i> , <i>oriR101</i> , <i>repA101</i> (Ts), <i>araC</i> -P _{araB} ⁻ -γ-β- <i>exo</i> (encode λ Red recombinases), temperature-conditional replicon	[30]
pKD13	<i>bla</i> , FRT- <i>kan</i> -FRT	[30]
pCP20	<i>FLP</i> ⁺ , λ cI857 ⁺ , λ P _R Pep ^{ts} , <i>bla</i> , <i>catF</i>	[31]
P _{BAD} - <i>his6-prkA</i> -pA CYC184	Recombinant plasmid carries <i>prkA</i> gene (derived from <i>Synechococcus</i> PCC7492) for the overexpression of phosphoribulokinase (PrkA) under the control of P _{BAD}	[13]
<i>rbclS</i> -pET30a + (M259T)	Recombinant plasmid carries engineered <i>rbclS</i> gene (originated from <i>Synechococcus</i> PCC6301) for the overexpression of engineered Rubisco (M259T) under the control of P _{T7}	[13]
<i>rbclS</i> -pET30a + (M259T, K198G)	Recombinant plasmid carries engineered <i>rbclS</i> gene (originated from <i>Synechococcus</i> PCC6301) for the overexpression of engineered Rubisco (M259T and K198G) under the control of P _{T7}	This study
<i>rbclS</i> -pET30a + (M259T, K198G, D200G, E201G)	Recombinant plasmid carries engineered <i>rbclS</i> gene (originated from <i>Synechococcus</i> PCC6301) for the overexpression of engineered Rubisco (M259T, K198G, D200G, and E201G) under the control of P _{T7}	This study
<i>rbclS</i> -pET30a + (M259T, K198G, K172G)	Recombinant plasmid carries engineered <i>rbclS</i> gene (originated from <i>Synechococcus</i> PCC6301) for the overexpression of engineered Rubisco (M259T, K198G, and K172G) under the control of P _{T7}	This study
<i>rbclS</i> -pET30a + (M259T, K198G, K331G)	Recombinant plasmid carries engineered <i>rbclS</i> gene (originated from <i>Synechococcus</i> PCC6301) for the overexpression of engineered Rubisco (M259T, K198G, and K331G) under the control of P _{T7}	This study

to occur when Rubisco is aerobically overexpressed in *E. coli* BL21 (DE3) [15] or anaerobically in *E. coli* MZ [16] and MZLFB (see results below). The enhanced anaplerosis competes with PTS for PEP. This may further intensify the activity of glycolysis and PTS and thus results in the enhanced pyruvate production.

A second pathway for the enhanced pyruvate accumulation by the presence of Rubisco can be argued as follows. Pyruvate should be primarily directed to the production of C-2 fermentation products since *ldh* and *frd* have been deactivated in *E. coli* MZLF. The anaerobic conversion of pyruvate to C-2 fermentation products is started by the enzymatic reaction catalyzed by pyruvate formate-lyase (PFL), where the reaction products are acetyl-CoA and formate. The enhanced pyruvate regulation may result from the down-regulation of the transcription of the *focA-pflB* operon and thus decrease the total activity of PFL. The regulation of gene

transcriptions involves a complex network of global and local regulators. In *E. coli*, the transcription of about one-half of genes is regulated by seven global regulators including ArcA, Crp, Fis, Fnr, Ihf, Lrp, and NarL [23]. It is known that the transcription of the *focA-pflB* operon is positively regulated by the redox-dependent transcriptional activators of FNR and ArcA [24, 25] whereas, ArcA is found to be critical to the transcription of the *focA-pflB* operon [25]. It is surprising to see that the transcriptional level of *arcA* (encodes the aerobic respiration control protein) is down-regulated in *E. coli* strains J3 and JB due to the presence of Rubisco, as noted in Table 2. This should also hold true when Rubisco is expressed in MZLF. Several studies have shown that the disruption of *arcA* in *E. coli* would activate the glyoxylate shunt [26, 27]. This is consistent with NGS data where the transcription levels of genes associated with the glyoxylate shunt were indeed enhanced, as shown in Additional file 1. The *arcA* mutant

Table 2 Transcriptional levels of global regulators in Rubisco-based *E. coli*

Global regulator	log ₂ Ratio in J3	log ₂ Ratio in JB
<i>arcA</i>	-0.81	-0.61

The definition of log₂Ratio can be found in Text S1. All log₂Ratio reported here are statistically significant where all p-values are less than 1×10^{-3} and all False Discovery Rates (FDRs) are less than 0.05

strain also exhibited a decrease in the acetate yield and an increase in biomass yield [26, 27]. These phenotypes of *arcA* mutant strain are consistent with our data as discussed here and below. Therefore, the down-regulation of *arcA* transcription provides a phenomenological explanation for the results of pyruvate accumulation where the transcription of the *focA-pflB* operon may decrease. More work is needed to elucidate the detailed mechanism of Rubisco-induced phenotypes.

Carbon dioxide is recycled and converted into fermentation products and biomass by Rubisco-based engineered pathway

With the elucidation of the Rubisco-induced responses, it is interesting to verify the carbon recovery and carbon distribution for *E. coli* containing Rubisco-based engineered pathway. It can be seen in Fig. 2a that while the carbon recovery for MZLF is 92 %, the carbon recovery for MZLFB and MZLFB + IP is 91 and 96 %, respectively. By including the contribution of pyruvate accumulation, the perplexing problem of low carbon recovery (ca. 70 %) during fermentation by *E. coli* containing Rubisco-based engineered pathway has been solved [15, 16]. Moreover, two important analyses can be made with good carbon recoveries. First, it is interesting to see a significant difference in the carbon distribution between strains MZLF and MZLFB + IP (Fig. 2b). In addition to the increase in pyruvate production, the molar yield of biomass increased from 0.37 to 0.52, and it is therefore suggested that Rubisco may be a key to stimulate bacterial growth. Second, it can be observed from Fig. 2b that the amount of carbons needed to match the increase in carbon yields of the biomass and pyruvate cannot be simply balanced by the decrease in the carbon yield of acetate alone. However, when C-1 compounds are taken into consideration, a good carbon balance during the carbon re-distribution between MZLF and MZLFB + IP can be made. Therefore, it is suggested that CO₂, derived from formate, will also be converted to the biomass and fermentation products in MZLFB + IP.

Considering the profile of fermentation products where C-3, C-2, and C-1 account for 83 and 86 % of total end metabolites for MZLFB and MZLFB + IP, respectively (Table 3), a reasonable conclusion is that glycolysis (Eq.

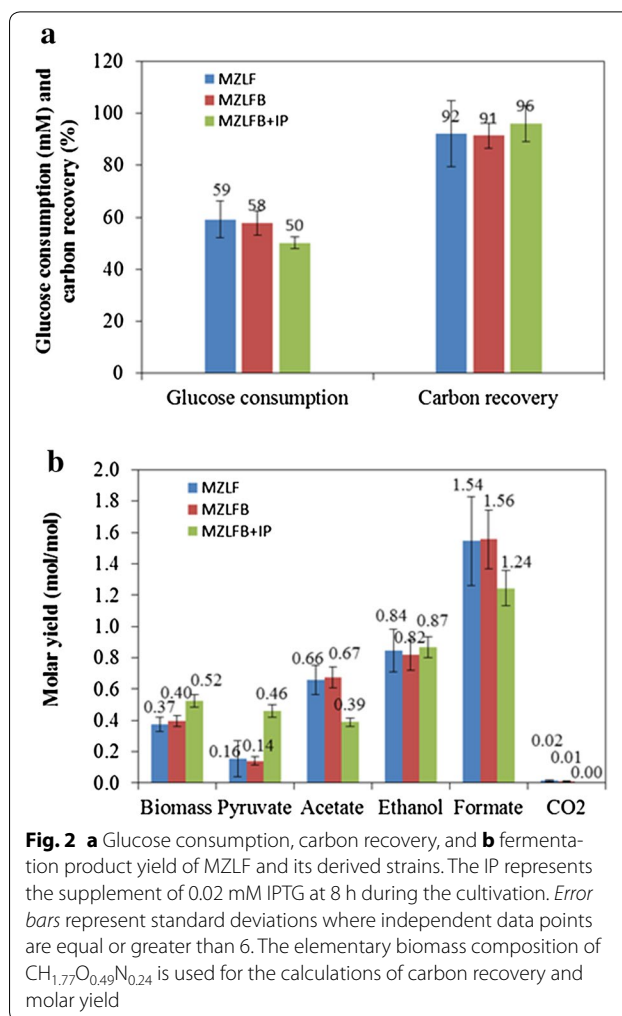


Fig. 2 a Glucose consumption, carbon recovery, and b fermentation product yield of MZLF and its derived strains. The IP represents the supplement of 0.02 mM IPTG at 8 h during the cultivation. Error bars represent standard deviations where independent data points are equal or greater than 6. The elementary biomass composition of CH_{1.77}O_{0.49}N_{0.24} is used for the calculations of carbon recovery and molar yield

(1), below) and subsequent C-2 fermentation routes (Eqs. 2 and 3, below) are the major metabolic fate for glucose. The 83 and 86 % of C-1, C-2, and C-3 metabolites are calculated from the data in Table 3 by taking pyruvate, acetate, ethanol, formate, and CO₂ into considerations for the calculation of the carbon recovery, whereas the lactate yield is small enough to be neglected. Two additional routes are appended to account for the activity of Rubisco-based engineered pathway (Eqs. 4 and 5, below). Since each equation has distinct stoichiometry for C-1 metabolism, where glycolysis produces zero C-1 (Eq. 1), conventional C-2 fermentation produces two C-1 (Eqs. 2 and 3), and the Rubisco-based engineered pathway produces 1.2 C-1 (Eqs. 4 and 5), the distribution of glucose flux among metabolic fates (Eqs. 1–5) for MZLFB can be simply determined by the profile of the end metabolite. In other words, the final concentrations of C-3, C-2, and C-1 metabolites are interdependent. Detailed derivations for Eqs. 1–5 are presented in Additional file 1.

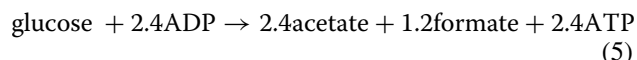
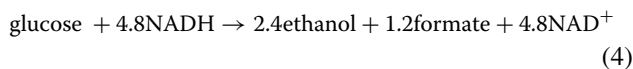
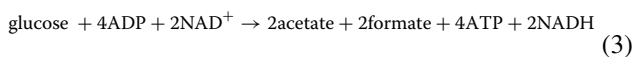
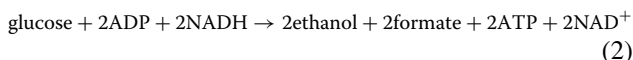
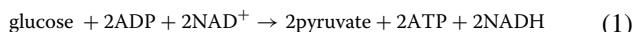
Table 3 Fermentation profiles of *E. coli* MZLF derived strains

<i>E. coli</i> strains	Glucose consumption (mM)	Molar yield (mmol/mmol)								Carbon recovery (%)
		Pyr	Ace	EtOH	Lac	Suc	For	CO ₂	Biomass	
MZLF	59 ± 7	0.16 ± 0.12	0.66 ± 0.09	0.84 ± 0.14	0.04 ± 0.02	0	1.54 ± 0.28	0.02 ± 0.005	0.37 ± 0.05	92 ± 9
MZLF3 + IP	55 ± 1	0.46 ± 0.02	0.41 ± 0.00	0.87 ± 0.01	0.03 ± 0.00	0	1.30 ± 0.02	0.001 ± 0.00	0.54 ± 0.02	98 ± 1
MZLFB	58 ± 5	0.14 ± 0.03	0.67 ± 0.07	0.82 ± 0.10	0.04 ± 0.01	0	1.56 ± 0.19	0.01 ± 0.003	0.40 ± 0.03	92 ± 5
MZLFB + IP	50 ± 2	0.46 ± 0.04	0.40 ± 0.03	0.87 ± 0.07	0.03 ± 0.01	0	1.24 ± 0.11	0	0.52 ± 0.04	96 ± 7
MZLFB + ace + IP	51 ± 1	0.61 ± 0.06	0.25 ± 0.05	0.82 ± 0.04	0.02 ± 0.0	0	1.13 ± 0.06	0	0.50 ± 0.03	94 ± 4

The calculation of carbon recovery includes ethanol, acetate, formate, lactate, succinate, malate, CO₂, and biomass. The elementary biomass composition of CH_{1.77}O_{0.49}N_{0.24} is used for the calculations of carbon recovery [18]

IP and ace represent the supplement of 0.05 mM IPTG and 30 mM acetate at 8 h during the cultivation

Pyr pyruvate, Ace acetate, EtOH ethanol, Lac lactate, Suc succinate, For formate



According to Eqs. 2–5, the theoretical C-2/C-1 ratio can be calculated as a function of the distribution of glucose flux between conventional fermentation route and Rubisco-based engineered pathway (Fig. 3a). When the C-2/C-1 ratio is 1, glucose flux to Rubisco-based engineered pathway should be 0 %. This scenario represents a conventional fermentation process as shown in Eqs. 2 and 3. The C-2/C-1 ratio non-linearly increases from 1 to 2 as the contribution of the Rubisco-based engineered pathway described by Eqs. 4 and 5 increases from 0 to 100 %. It can be seen in Fig. 3b that the experimental data showed that C-2/C-1 for MZLF was 0.96. With the addition of 0.02 mM IPTG to increase the expression of Rubisco in MZLFB, the molar ratio of C-2/C-1 increased to 1.01. This indicates that in addition to conventional C-2 fermentation routes (Eqs. 2 and 3), Rubisco-based engineered pathway should participate in C-2 fermentative production as given by Eqs. 4 and 5. Furthermore, the 5 % increase in the molar ratio of C-2/C-1 for MZLFB + IP corresponds with roughly 9 % of the glucose flux flow into

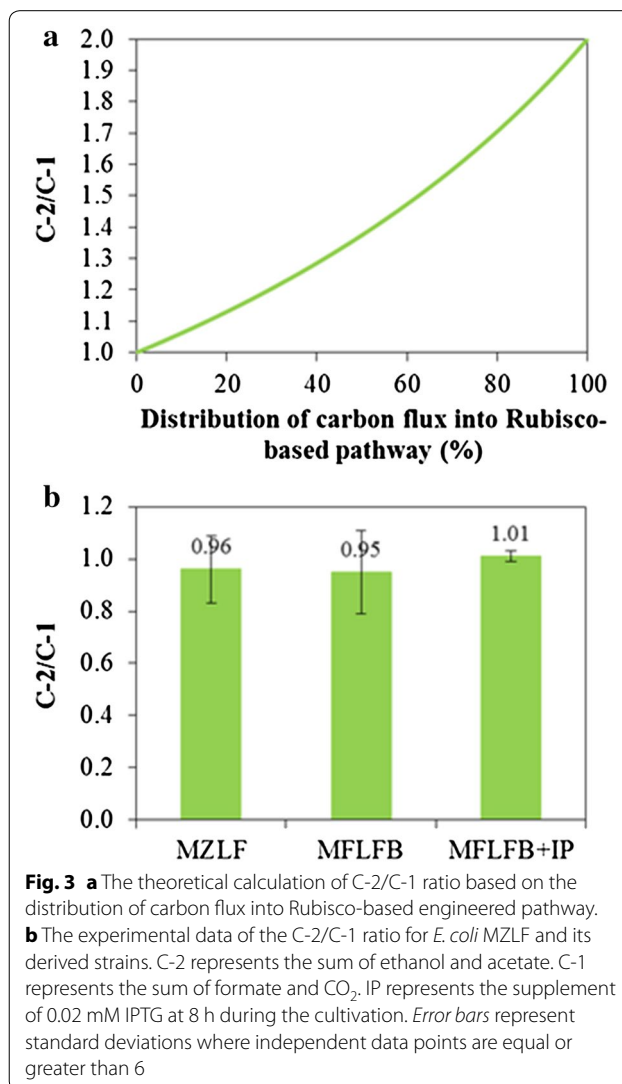


Fig. 3 a The theoretical calculation of C-2/C-1 ratio based on the distribution of carbon flux into Rubisco-based engineered pathway. **b** The experimental data of the C-2/C-1 ratio for *E. coli* MZLF and its derived strains. C-2 represents the sum of ethanol and acetate. C-1 represents the sum of formate and CO₂. IP represents the supplement of 0.02 mM IPTG at 8 h during the cultivation. Error bars represent standard deviations where independent data points are equal or greater than 6

Rubisco-based engineered pathway. This corresponds to C-2/C-1 of 1.05 which is a 5 % increase compared to the base whose C-2/C-1 is 1.00. The deviation of C-2/C-1 for MZLF from the theoretical calculation can be attributed to the fact that CO₂ evolved from the production of biomass is included in the calculation of C-2/C-1. The percentage of the carbon flux directing into Rubisco-based engineered pathway is therefore under-estimated. Note that it was proposed that 2.8 mol of CO₂ would be evolved when one mole of biomass was produced [26].

To verify the *in vivo* activity of Rubisco-based engineered pathway, two Rubisco mutants were prepared to replace the parental Rubisco in MZLFB. The first Rubisco mutant was Rubisco (K198G) where the lysine at the position 198 is the essential binding site for CO₂ [28]. The second Rubisco mutant was prepared by introducing additional amino acid substitution to get Rubisco (K198G, K172G). The lysine at the position 172 is associated with the binding of ribulose-1,5-bisphosphate [28]. While the molar ratio of C-2/C-1 for MZLF was 0.96, the increase in the C-2/C-1 ratio to 1.01 for MZLFB + IP demonstrated the proper function of Rubisco-based engineered pathway. When Rubisco(K198G) was substituted for parental Rubisco, a dramatic decrease in the C-2/C-1 ratio to 0.86 was observed (Fig. 4a). It can be seen that Rubisco with double mutations of K198G and K172G had the C-2/C-1 ratio of 0.83, which is also far below the performance of MZLFB + IP. This control experiment demonstrates the *in vivo* activity of Rubisco-based engineered pathway. Thus, the Rubisco-based engineered pathway can be deactivated by mutating

lysine at position 198 of the primary structure. Note that the overexpression of Rubisco (K198G) can be confirmed by SDS-PAGE as shown in Additional file 1. Also noted was that the overexpression of Rubisco (K198G) also enhanced the accumulation of pyruvate (Fig. 4b). This indicates that the enhanced pyruvate accumulation is not caused by the carboxylation reaction catalyzed by Rubisco.

The feasibility of mixotrophic *E. coli* as a platform for bio-based chemical productions

The feasibility of mixotrophic *E. coli* has been demonstrated (see Fig. 5a). It is well known that the expression of PrkA in *E. coli* is a burden for bacterial growth yet the co-expression of Rubisco can alleviate such retarded growth [13, 15, 16]. These previous studies can be illuminated not only with respect to carbon flow but also to the intracellular energy balance. It can be seen that in a regime where 9 % of the carbon is directed into Rubisco-based engineered pathway, the energy can still be self-balancing while CO₂ is recycled. In such case, the growths of MZLFB and MZLB + IP were comparable or even better than that of wild-type *E. coli*. This is consistent with our previous suggestion of the compatibility of Rubisco-based engineered pathway with the central metabolism of *E. coli* [16]. Moreover, there is plenty of formate (1.24 mol/mole glucose) after directing 9 % of the carbon to Rubisco-based engineered pathway, indicating that energy may not be a constraint for the further forcing of even more carbon into Rubisco based engineered pathway.

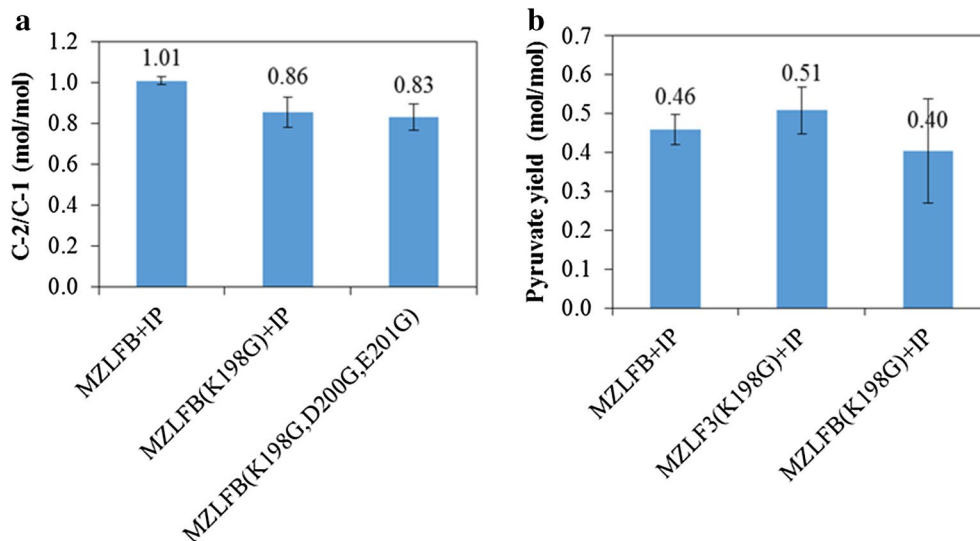
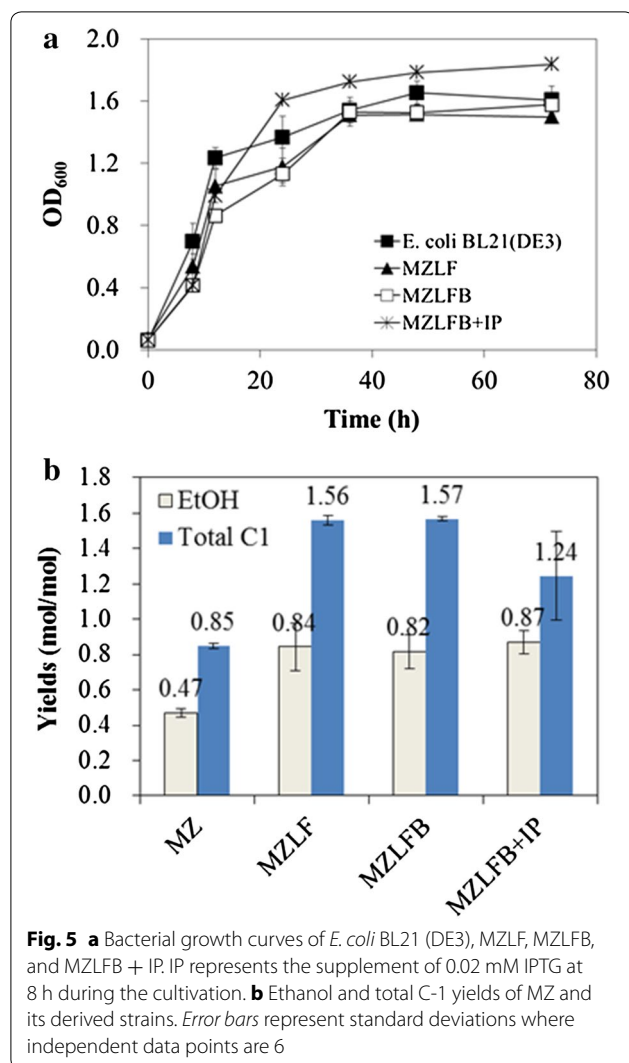


Fig. 4 **a** C-2/C-1 ratios of MZLF, MZLFB, MZLFB (K198G), and MZLFB (K198G,K172G). **b** Pyruvate yields of MZLFB + IP, MZLF3 (K198G) + IP, and MZLFB (K198G) + IP. Error bars represent standard deviations where independent data points are equal or greater than 3



The feasibility of mixotrophic *E. coli* can also be perceived by examining ethanol production and the associated C-1 accumulation. It can be seen in Fig. 5b that *E. coli* strain MZ produced 0.47 mol-ethanol/mol-glucose with a 0.85 mol-C-1/mol-glucose. By de-activating *ldh* and *frd* genes from MZ, *E. coli* strain MZLF produced 0.84 mol-ethanol/mol-glucose (79 % increase) while C-1 production was proportionally increased to 1.56 mol-C-1/mol-glucose. The introduction of Rubisco-based engineered pathway into MZLF enhanced the ethanol production by 4 % while decreasing total C-1 production by 21 %. This is in agreement with the theoretical calculation that 9 % of carbon flux was directed into Rubisco-based engineered pathway. Note that some recycled C-1 could arguably become biomass since the biomass yield increase from 0.37 for MZLF to 0.52 for MZLFB + IP.

Conclusions

Here, we report for the first time the complete profile of fermentation products using *E. coli* MZLF and its derived strains. The profiles reveal that the heterologous expression of form I Rubisco has a strong impact on the central metabolism of a non-phototrophic heterotroph *E. coli*, resulting in significant increases in the production of biomass and pyruvate. By examining the comprehensive profile of fermentation products, it is estimated that 9 % of glucose consumption is directed from glycolysis to Rubisco-based engineered pathway. The co-existence of glycolysis and Rubisco-based engineered pathway in *E. coli* MZLFB poses an example as the mixotroph where the principle characteristics of MZLFB are the high bacterial growth and the low CO₂ emission.

Methods

Bacterial strains and plasmids

All strains and plasmids used in this study are listed in Table 1. The *ldh* gene knock-out mutant derived from *E. coli* strain MZ and the *frd* gene knock-out mutant derived from *E. coli* strain MZL were constructed through the one-step inactivation procedure [29, 30]. The sequences of primers used for the synthesis of linear DNA fragments for Red-mediated recombination can be found in Additional file 1. More information regarding the construction of mutant strains can be found in [16].

The recombinant plasmid *rbclS*-pET30a + (M259T,K198G) was derived from *rbclS*-pET30a + (M259T) by the Q5 Site-Directed Mutagenesis Kit (New England BioLabs® Inc., the USA), where primers *rbcl*-K198G-F and *rbcl*-K198G-R were used, see Additional file 1. *rbclS*-pET30a + (M259T,K198G,D200G,E201G), *rbclS*-pET30a + (M259T,K198G,K172G), and *rbclS*-pET30a + (M259T,K198G,K331G) were generated subsequently from *rbclS*-pET30a + (M259T,K198G). Four recombinant plasmids were subject to DNA sequencing (serviced by Biotechnology center at National Chung Hsing University, Taiwan). All primers used for the amplification of mutation were listed in (Additional file 1).

Culture media and growth conditions

Escherichia coli strains used for fermentation study were grown anaerobically at 200 rpm and 37 °C in fresh 25-ml M9 defined medium containing (per liter): 12.8 g Na₂HPO₄·7 H₂O; 3 g KH₂PO₄; 0.5 g NaCl; 1.0 g NH₄Cl; 0.24 g MgSO₄; 0.011 g CaCl₂; and 20 g glucose. An anaerobic culture environment was achieved in a sealed serum bottle as described previously [31]. Initial OD₆₀₀ was adjusted to 0.05. The pH was adjusted to 8

at the fermentation times of 0, 8, and 24 h. The respective concentrations of streptomycin, chloramphenicol and kanamycin used were 50, 34, and 50 µg/ml. The isopropyl-β-D-1-thiogalactopyranoside (IPTG) and acetate was added at 8 h when needed.

Analytical methods

The cell density was measured at 600 nm using a UV-Vis spectrophotometer (GENESYS 10S, Thermo Scientific, USA). The gaseous CO₂ concentration in the headspace of the cultures was measured by a diffusive infrared-based CO₂ analyzer (Sentry ST303). The total CO₂ concentration was calculated based on the gaseous CO₂ concentration and the detailed calculation has been described in [15, 16].

Samples for quantification of residual glucose or extracellular metabolites were collected from the culture solutions followed by the centrifugation for 5 min at 17,000×g to remove cell pellets. The supernatant was filtered by a 0.2 µm PVDF filter before sample injection. The concentration of residual glucose was determined by either HPLC or DNS methods [32]. Characterization and quantification of extra-cellular formate, acetate, ethanol, lactate, succinate, and pyruvate were performed by Thermo Scientific™ Dionex™ Ultimate 3000 LC Systems. The separation of the mixture was achieved with the HPLC column Thermo scientific HyperREZ XP Carbohydrate H⁺ (300 mm × 7.7 mm 8 µm) where the measurement was done with a refractive index (RI) detector. The mobile phase was 5 mM H₂SO₄. The temperature was maintained at 65 °C while the flow rate was maintained at 1.0 ml per minute. The sample injection was done by an autosampler whereas the injection volume is 20 µl.

The qualitative and quantitative analysis of pyruvate was further confirmed by the use of Pyruvate Colorimetric/Fluorometric Assay Kit (Biovision Inc., the USA). Basically, 50 µl proprietary Reaction Mix, containing 46 µl of Assay Buffer, 2 µl of Pyruvate Probe, and 2 µl Enzyme Mix, were mixed with 50 µl of sample. Incubate the mixtures in a light-free condition for 30 min at room temperature. The absorbance of samples at 570 nm was measured using a microplate reader.

Quantification of mRNA expression level

The RNA sequencing was done by Genomics BioSci & Tech Ltd and used to quantify the expression level of mRNA. Primary sequencing data of cDNA library were performed by Illumina HiSeq™ 2000 and the data mapping was done with SOAPaligner/SOAP2. *E. coli* strains J3 together with *E. coli* BL21 (DE3) as the control experiment were aerobic cultivated in LB medium supplemented with 20 g/l L-arabinose [15]. Meanwhile, *E. coli*

strains JB together with *E. coli* BL21 (DE3) as the control experiment were anaerobic cultivated in M9 medium supplemented with 20 g/l D-glucose as presented above. The samples for J3 transcriptome analysis were collected at 24 h while the samples for JB transcriptome analysis were collected at 24 h. Four samples for RNA-seq were shipped out with dry ice bath. Detailed protocol for sample preparation, RNA-seq, and data analysis can be found in Text S1 and [16].

Additional files

Additional file 1. Supplemental Materials and Methods.

Abbreviations

The CBB cycle: The Calvin–Benson–Bassham cycle; PRK: phosphoribulokinase; PrkA: phosphoribulokinase originated from *Synechococcus* PCC7492; Rubisco: Ribulose-1,5-bisphosphate carboxylase/oxygenase; RDE: Rubisco-dependent *Escherichia coli*; C-1 compounds: represent formate and CO₂; C-2 compounds: represent ethanol and acetate; PFL: pyruvate formate-lyase; ArcA: aerobic respiration control protein; SDS-PAGE: sodium dodecyl sulfate–polyacrylamide gel electrophoresis; IPTG: isopropyl-β-D-1-thiogalactopyranoside.

Authors' contributions

CHY constructed recombinant strains and plasmids, carried out the fermentation experiments, and analyzed fermentation and RNA-seq data. EJJ carried out the fermentation experiments and analyzed fermentation and RNA-seq data. YLC constructed recombinant plasmids for expressing mutant Rubiscos and carried out fermentation experiments. FYOY carried out the fermentation experiments and analyzed RNA-seq data. SYL conceived and designed research, analyzed data, and wrote the manuscript. All authors read and approved the final manuscript.

Acknowledgements

This work was funded by the Ministry of Science and Technology Taiwan.

Competing interests

The authors declare that they have no competing interests.

Availability of data and materials

The datasets supporting the conclusions of this article are included within the article and its supplementary materials.

Consent for publication

Not applicable.

Ethics approval and consent to participate

Not applicable.

Funding

This work was funded by the Ministry of Science and Technology Taiwan, MOST-103-2221-E-005-072-MY3 and MOST-104-2621-M-005 -004 -MY3.

Received: 21 January 2016 Accepted: 21 July 2016

Published online: 02 August 2016

References

- Martin W, Schnarrenberger C. The evolution of the Calvin cycle from prokaryotic to eukaryotic chromosomes: a case study of functional redundancy in ancient pathways through endosymbiosis. *Curr Genet*. 1997;32:1–18.

2. Bauwe H, Hagemann M, Kern R, Timm S. Photorespiration has a dual origin and manifold links to central metabolism. *Curr Opin Plant Biol*. 2012;15:269–75.
3. Ho S-H, Li P-J, Liu C-C, Chang J-S. Bioprocess development on microalgae-based CO₂ fixation and bioethanol production using *Scenedesmus obliquus* CNW-N. *Bioresour Technol*. 2013;145:142–9.
4. Lo Y-C, Chen C-Y, Lee C-M, Chang J-S. Sequential dark–photo fermentation and autotrophic microalgal growth for high-yield and CO₂-free biohydrogen production. *Int J Hydrogen Energy*. 2010;35:10944–53.
5. Atsumi S, Higashide W, Liao JC. Direct photosynthetic recycling of carbon dioxide to isobutyraldehyde. *Nat Biotech*. 2009;27:1177–80.
6. Gao Z, Zhao H, Li Z, Tan X, Lu X. Photosynthetic production of ethanol from carbon dioxide in genetically engineered cyanobacteria. *Energy Environ Sci*. 2012;5:9857–65.
7. Lan EI, Liao JC. Metabolic engineering of cyanobacteria for 1-butanol production from carbon dioxide. *Metab Eng*. 2011;13:353–63.
8. Angermayr SA, GorchsRovira A, Hellingwerf KJ. Metabolic engineering of cyanobacteria for the synthesis of commodity products. *Trends Biotechnol*. 2015;33:352–61.
9. Schwender J, Goffman F, Ohlrogge JB, Shachar-Hill Y. Rubisco without the Calvin cycle improves the carbon efficiency of developing green seeds. *Nature*. 2004;432:779–82.
10. Greene DN, Whitney SM, Matsumura I. Artificially evolved *Synechococcus* PCC6301 Rubisco variants exhibit improvements in folding and catalytic efficiency. *Biochem J*. 2007;404:517–24.
11. Mueller-Cajar O, Morell M, Whitney SM. Directed evolution of rubisco in *Escherichia coli* reveals a specificity-determining hydrogen bond in the form II enzyme. *Biochemistry*. 2007;46:14067–74.
12. Mueller-cajar O, Whitney SM. Evolving improved *Synechococcus Rubisco* functional expression in *Escherichia coli*. *Biochem J*. 2008;414:205–14.
13. Parikh MR, Greene DN, Woods KK, Matsumura I. Directed evolution of RuBisCO hypermorphs through genetic selection in engineered *E. coli*. *Protein Eng Des Sel*. 2006;19:113–9.
14. Gong F, Liu G, Zhai X, Zhou J, Cai Z, Li Y. Quantitative analysis of an engineered CO₂-fixing *Escherichia coli* reveals great potential of heterotrophic CO₂ fixation. *Biotechnol Biofuels*. 2015;8:86.
15. Zhuang Z-Y, Li S-Y. Rubisco-based engineered *Escherichia coli* for in situ carbon dioxide recycling. *Bioresour Technol*. 2013;150:79–88.
16. Li Y-H, Ou-Yang F-Y, Yang C-H, Li S-Y. The coupling of glycolysis and the Rubisco-based pathway through the non-oxidative pentose phosphate pathway to achieve low carbon dioxide emission fermentation. *Bioresour Technol*. 2015;187:189–97.
17. Guadalupe-Medina V, Wisselink H, Luttik M, de Hulster E, Daran J-M, Pronk J, van Maris A. Carbon dioxide fixation by Calvin-Cycle enzymes improves ethanol yield in yeast. *Biotechnol Biofuels*. 2013;6:125.
18. Grosz R, Stephanopoulos G. Statistical mechanical estimation of the free energy of formation of *E. coli* biomass for use with macroscopic bioreactor balances. *Biotechnol Bioeng*. 1983;25:2149–63.
19. Koebmann BJ, Westerhoff HV, Snoep JL, Nilsson D, Jensen PR. The glycolytic flux in *Escherichia coli* is controlled by the demand for atp. *J Bacteriol*. 2002;184:3909–16.
20. Causey TB, Shanmugam KT, Yomano LP, Ingram LO. Engineering *Escherichia coli* for efficient conversion of glucose to pyruvate. *Proc Natl Acad Sci USA*. 2004;101:2235–40.
21. Wang Q, Ou MS, Kim Y, Ingram LO, Shanmugam KT. Metabolic flux control at the pyruvate node in an anaerobic *Escherichia coli* strain with an active pyruvate dehydrogenase. *Appl Environ Microbiol*. 2010;76:2107–14.
22. Sauer U, Eikmanns BJ. The PEP—pyruvate—oxaloacetate node as the switch point for carbon flux distribution in bacteria: We dedicate this paper to Rudolf K. Thauer, Director of the Max-Planck-Institute for Terrestrial Microbiology in Marburg, Germany, on the occasion of his 65t. *FEMS Microbiol Rev* 2005, 29:765–94.
23. Martinez-Antonio A, Collado-Vides J. Identifying global regulators in transcriptional regulatory networks in bacteria. *Opin Microbiol*. 2003;6:482–9.
24. Sawers RG. Differential turnover of the multiple processed transcripts of the *Escherichia coli* fcaA-pflB operon. *Microbiology*. 2006;152:2197–205.
25. Sawers G, Suppmann B. Anaerobic induction of pyruvate formate-lyase gene expression is mediated by the ArcA and FNR proteins. *J Bacteriol*. 1992;174:3474–8.
26. Nikel PI, Zhu J, San K-Y, Méndez BS, Bennett GN. Metabolic flux analysis of *Escherichia coli* creB and arca mutants reveals shared control of carbon catabolism under microaerobic growth conditions. *J Bacteriol*. 2009;191:5538–48.
27. Waegeman H, Beauprez J, Moens H, Maertens J, De Mey M, Foulquié-Moreno M, Heijnen J, Charlier D, Soetaert W. Effect of iclR and arca knockouts on biomass formation and metabolic fluxes in *Escherichia coli* K12 and its implications on understanding the metabolism of *Escherichia coli* BL21 (DE3). *BMC Microbiol*. 2011;11:1–17.
28. Shinozaki K, Yamada C, Takahata N, Sugiura M. Molecular cloning and sequence analysis of the cyanobacterial gene for the large subunit of ribulose-1,5-bisphosphate carboxylase/oxygenase. *Proc Natl Acad Sci USA*. 1983;80:4050–4.
29. Datsenko KA, Wanner BL. One-step inactivation of chromosomal genes in *Escherichia coli* K-12 using PCR products. *Proc Natl Acad Sci USA*. 2000;97:6640–5.
30. Cherepanov PP, Wackernagel W. Gene disruption in *Escherichia coli*: TcR and KmR cassettes with the option of FLP-catalyzed excision of the antibiotic-resistance determinant. *Gene*. 1995;158:9–14.
31. Chen S-K, Chin W-C, Tsuge K, Huang C-C, Li S-Y. Fermentation approach for enhancing 1-butanol production using engineered butanogenic *Escherichia coli*. *Bioresour Technol*. 2013;145:204–9.
32. Miller GL. Use of dinitrosalicylic acid reagent for determination of reducing sugar. *Anal Chem*. 1959;31:426–8.

Submit your next manuscript to BioMed Central and we will help you at every step:

- We accept pre-submission inquiries
- Our selector tool helps you to find the most relevant journal
- We provide round the clock customer support
- Convenient online submission
- Thorough peer review
- Inclusion in PubMed and all major indexing services
- Maximum visibility for your research

Submit your manuscript at
www.biomedcentral.com/submit

